Pulsed Single-Mode Yb-Doped Fibre Amplifier around 976 nm: Numerical Modelling and Experimental Study

Aude Bouchier[a,b], Mikhaël Myara[c], Gaëlle Lucas-Leclin[d], Patrick Georges[d]

[a] CNRS ; LAAS ; 7 avenue du colonel Roche, F-31077 Toulouse, France;
[b] Université de Toulouse ; UPS, INSA, INP, ISAE ; LAAS ; F-31077 Toulouse, France;
[c] Institut d'Electronique du Sud UMR5214, Université de Montpellier 2, 34095 Montpellier cedex 5, France;
[d] Laboratoire Charles Fabry de l'Institut d'Optique, CNRS UMR 8501, Univ. Paris-Sud, Campus Polytechnique, RD 128, 91127 Palaiseau Cedex, France

ABSTRACT

Diffraction-limited sources around $976\ nm$ are attractive to build sources around $488\ nm$, or to pump rare-earth-doped materials. Continuous wave efficient lasers have been obtained with single-mode fibres, in which we demonstrate pulsed laser diode amplification with gains higher than $30\ dB$. Theoretical studies can predict the amplifier performances versus the input signal characteristics and show the pulse width influence on excited state population. We used a classical time-space two-level model that we solved thanks to a Finite-Difference Time-Domain method. These simulations taking into account both time and space evolutions and a parasitic laser effect describe correctly the experimental results.

Keywords: Yb-doped fibre amplifier, time and space modelisation, FDTD method

1. INTRODUCTION

High power diffraction-limited sources around 976 nm are attractive to build new sources around $488\ nm$ with a non linear stage, or to propose pump sources for rare-earth-doped materials. Solutions based on semiconductor devices are proposed with extended cavity laser diodes[1] or optically pumped semiconductor lasers.[2] Among other solutions, ytterbium-doped materials present high emission cross-section around $976\ nm$, which can be used with a pumping around $915\ nm$.

The main difficulty of this transition is its true three-level behaviour corresponding to a strong absorption at the emission wavelength. We thus need pump laser sources at $915\ nm$ bright enough to reach the transparency intensity of the active area and overcome the ground-state absorption that is difficult to obtain in a bulk crystal. That's why, although laser emission at $981\ nm$ in Yb:KYW[3] and at $985\ nm$ in Yb:S-FAP[4] bulk crystals have been demonstrated under Ti:Sapphire pumping, most of the experiments have been reported with Yb-doped fibres. Fibres effectively enable a long interaction and a good overlap of the propagating beams with the active core.

With these lasers based on Yb-doped fibres, the frequency conversion to blue emission is achieved in extracavity configuration and CW regime thanks to high efficiency non linear materials such as BIBO bulk crystals, with a power of $15\ mW$[5] or PPLN waveguides with a power of $83\ mW$.[6]

The pulsed regime is a possible way to increase nonlinear frequency conversions efficiency. Pulsed sources at $976\ nm$, based on Yb-doped fibres, can be Q-switched[7] or mode-locked[8] sources. In this paper we study a master oscillator power amplifier configuration. A laser diode in gain-switch regime is thus amplified thanks to a single-mode (SM) doped fibre. This regime allows the choice of the repetition rate and the pulses duration. The criteria of choice for these two parameters are the signal input average power, in order to obtain a high gain, and the time domain shape of the amplified pulses.

We thus present an experimental and theoretical study of a pulsed laser diode amplification thanks to a SM Yb-doped fibre.The fibre has a core diameter of $5\ \mu m$ and a numerical aperture of 0.13 (INO - Canada). The Yb^{3+} ions concentration has been determined to be 4.8×10^{25} ions per m^3 thanks to pump absorption measurements. Both fibre ends are angle cleaved to avoid back reflections and parasitic laser effects.

email : bouchier@laas.fr, myara@opto.univ-montp2.fr

2. AMPLIFIER DESIGN

2.1 Choice of the Yb-doped Fibre

For silica fibres pumped around $915\ nm$, the transparency intensity is about $29\ kW/cm^2$ at $976\ nm$. With a bright pump laser source and a short enough fibre, reabsorption around this wavelength and emission around $1030\ nm$ can be avoided. Efficient continuous wave (CW) lasers made with single-mode Yb-doped fibres have been demonstrated at $974\ nm$[9] or $980\ nm$ with a $946 - nm$ Nd:YAG pump laser,[10] or at $977\ nm$ with a Nd:YVO_4 pump laser.[11]

To increase the laser emitted power for this transition, double-clad (DC) fibres have been developped. The overlap factor between the pump beam and the doped core for a DC fibre with a pump cladding of $120\ \mu m$ is $0.2\ \%$ leading to a transparency power close to $5\ W$ around $915\ nm$. To decrease this transparency power, specific double-clad fibres have been also developed, like jacketed-air-clad (JAC) fibres with a small inner-cladding to doped core ratio and a high numerical aperture, or rod-type DC fibres. Although high powers have been demonstrated in laser[12,13] and amplifier[14]configurations, these sources suffer from a limited absorption of the pump, a high transparency power and a complex fibre structure. Specific high-brightness multimode laser diodes modules for pumping remain also necessary.

For our study, we have used commercial single-mode fibers, which benefit from an intrinsic very good overlap of the pump beam with the doped core and thus a low transparency power. For our single-mode doped fiber, which charateristics are given in the introduction, the overlap factor between the pump and the doped core is $77\ \%$, leading to a transparency power as low as $7\ mW$. The fibres are pumped at $914\ nm$, which is very close to the highest absorption wavelength in the $870 - 960\ nm$ absorption band of Yb^{3+} ions.

2.2 Amplifier Set-Up

The experimental set-up is described in figure 1.

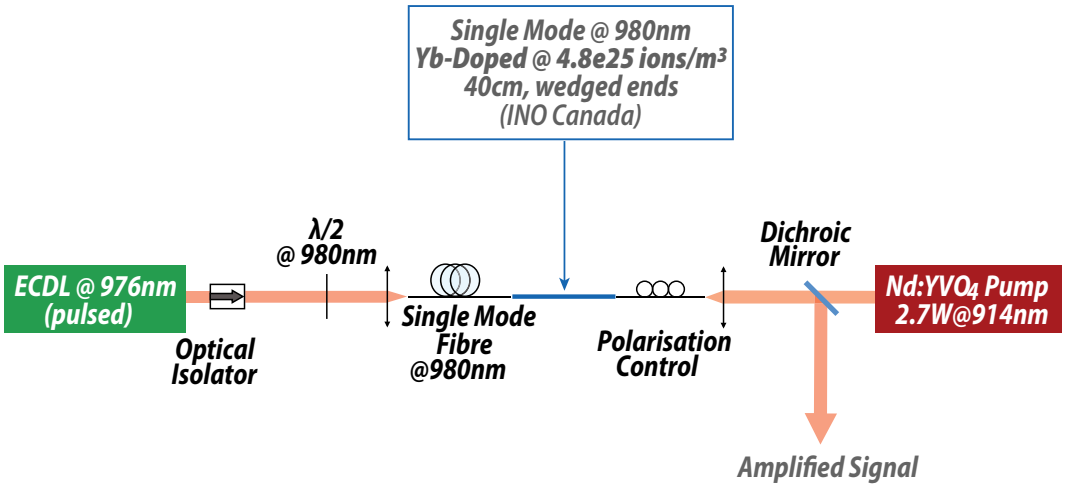

Figure 1. Amplifier Design

To pump these SM fibres, we developed a nearly diffraction-limited laser emitting $4\ W$ at $914\ nm$, based on the quasi-three level transition in a Nd:YVO_4 crystal. $3\ W$ are available at the doped fibre input. This laser is fully described in previous works.[6] For frequency conversion applications, the seed source bandwidth has to be narrower than nonlinear crystal spectral acceptance.

We thus developed a laser diode in external cavity, based on a transverse SM laser diode emitting around $976\ nm$ and a diffraction grating, with a spectral width as narrow as $0.3\ nm$ in pulsed operation. This regime is obtained thanks to the bias current modulation with pulse duration from $10\ ns$ to $100\ ns$, and repetition rates from $10\ kHz$ to $100\ MHz$. The launched pulses have an average power higher than $0.1\ mW$ and a peak power of $7\ mW$.

3. THEORETICAL STUDY : FDTD SIMULATIONS

3.1 Yb Amplifier Model

The true three-level transition we study here occurs between the wide ${}^2F_{7/2}$ and ${}^2F_{5/2}$ levels in Yb^{3+} ions. Because of the negligible non radiative lifetime of the excited state, this transition is modelled thanks to a two-level one (fig.2).

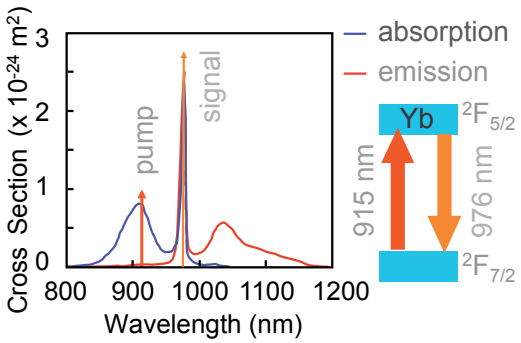

Figure 2. Yb^{3+} cross sections and two-level model

Excited atoms density, pump, signal and amplified spontaneous emission (ASE) around 976 nm propagations have been simulated with a very classical time-space two-level model,[15] well described by the following equations set :

$$\begin{cases} \left[\frac{n}{c}\frac{\partial}{\partial t}+\frac{\partial}{\partial z}\right]P_p(z,t) = \Gamma_p P_p\left((\sigma_p^{abs}+\sigma_p^{em})N_2-\sigma_p^{abs}N_{tot}\right) \\ \left[\frac{n}{c}\frac{\partial}{\partial t}+\frac{\partial}{\partial z}\right]P_s(z,t) = \Gamma_s P_s\left((\sigma_s^{abs}+\sigma_s^{em})N_2-\sigma_s^{abs}N_{tot}\right) \\ \left[\frac{n}{c}\frac{\partial}{\partial t}+\frac{\partial}{\partial z}\right]P_+(z,t) = \Gamma_s P_+\left((\sigma_s^{abs}+\sigma_s^{em})N_2-\sigma_s^{abs}N_{tot}\right)+\Gamma_s N_2\sigma_s^{em}\frac{2hc^2\delta\lambda}{\lambda_s^3} \\ \left[\frac{n}{c}\frac{\partial}{\partial t}-\frac{\partial}{\partial z}\right]P_-(z,t) = -\Gamma_s P_-\left((\sigma_s^{abs}+\sigma_s^{em})N_2-\sigma_s^{abs}N_{tot}\right)-\Gamma_s N_2\sigma_s^{em}\frac{2hc^2\delta\lambda}{\lambda_s^3} \\ \frac{\partial N_2}{\partial t} = (\eta_p P_p+\eta_s P_s+\eta_s P_+ +\eta_s P_-)\left(\sigma_p^{abs}N_{tot}-(\sigma_p^{abs}+\sigma_p^{em})N_2\right)-\frac{N_2}{\tau} \end{cases} \quad (1)$$

with P_p the pump power, P_s the signal power, P_+ the co-propagating ASE, P_- the counter-propagating ASE, and N_2 the amount of atoms on the excited state. η_p and η_s are defined by the following expressions :

$$\eta_p = \frac{\lambda_p\Gamma_p}{hcA_{eff}} \quad (2)$$

$$\eta_s = \frac{\lambda_s\Gamma_s}{hcA_{eff}} \quad (3)$$

All the other parameters are sumed-up in table 1.

The initial conditions are the following :

$$N_2(t=0,z=0) = 0 \quad (4)$$

$$P_p(t=0,z=0) = P_{p0} \quad (5)$$

$$P_p(t,z=0) = H(t-T+\Delta T)-H(t-T) \quad (6)$$

$$P_+(t=0,z=0) = 0 \quad (7)$$

$$P_-(t=0,z=L) = 0 \quad (8)$$

Symbol	Description	Value	Unit
Γ_p	Overlap Factor at pump wavelength	0.77	-
σ_p^{abs}	Absorption cross section at pump wavelength	0.74	pm^{-2}
σ_p^{em}	Emission cross section at pump wavelength	0	m^{-2}
λ_p	Pump Wavelength	915	nm
Γ_s	Overlap Factor at signal wavelength	0.74	-
σ_s^{abs}	Absorption cross section at signal wavelength	1.5	pm^{-2}
σ_s^{em}	Emission cross section at signal wavelength	1.9	pm^{-2}
λ_s	Signal Wavelength	976	nm
N_{tot}	Doping Level	4.8×10^{25}	m^{-3}
A_{eff}	Optical Fibre Effective Area	1.96×10^{-11}	m^2
λ_{ASE}	ASE wavelength	976	nm
$\delta\lambda$	ASE bandwidth	3	nm
R_1	Reflection Coefficient at left fibre end	10^{-6}	-
R_2	Reflection Coefficient at right fibre end	10^{-6}	-
L_1	Transmission Coefficient at left fibre end	1	-
L_2	Transmission Coefficient at right fibre end	1	-

Table 1. Sum-up of all the parameters for equation set 1.

with L the length of the optical fiber, T the period of the pulses at the input of the amplifier, ΔT the width of a pulse and $H(t)$ the Heaviside function. To take into account the parasitic laser effect on the ASE, some extremum conditions were added :

$$P_+(t, z = 0) = R_1(1 - L_1)^2 P_-(t, z = 0) \quad (9)$$

$$P_-(t, z = L) = R_2(1 - L_2)^2 P_+(t, z = L) \quad (10)$$

For this parasitic laser effect, we neglect the fibre ends losses, and consider that the tranmissions L_1 and L_2 are equal to unity.

3.2 Solving the Equations

However, because of the computation time required using traditionnal mathematic software, such a system is never solved numerically. We solved it thanks to a finite-difference time-domain (FDTD) method written for this purpose in optimised C++ langage to dramatically reduce the computation time. The spatio-temporal approach has been preferred to a pure time domain model, which strongly depends on hard to obtain spontaneous emission factors[16] .

The numerical expressions of the FDTD were easily obtained from eq.1 by using the centered-derivative approximations[17] . The overall numerical scheme were stabilized by using the Courant-Friedrichs-Lewy (CFL) condition[18] and allowed to define relationships between z and t steps.

Solving this system from standard initial conditions, i.e. considering 0 excited atom and a null ASE power for both co- and counter-propagating powers at $t = 0$, leads to a huge amount of time steps to reach the permanent regime. To strongly reduce the time spent during this phase, we used for initial conditions the result of a steady-state simulation, using the average pulsed signal power as input signal value. This leads to solve as a preliminary to the spatio-temporal simulation

the following equations system :

$$\begin{cases} \dfrac{\partial P_p(z)}{\partial t} = \Gamma_p P_p \left((\sigma_p^{abs} + \sigma_p^{em}) N_2 - \sigma_p^{abs} N_{tot} \right) \\ \dfrac{\partial P_s(z)}{\partial t} = \Gamma_s P_s \left((\sigma_s^{abs} + \sigma_s^{em}) N_2 - \sigma_s^{abs} N_{tot} \right) \\ \dfrac{\partial P_+(z)}{\partial t} = \Gamma_s P_+ \left((\sigma_s^{abs} + \sigma_s^{em}) N_2 - \sigma_s^{abs} N_{tot} \right) + \Gamma_s N_2 \sigma_s^{em} \dfrac{2hc^2 \delta\lambda}{\lambda_s^3} \\ \dfrac{\partial P_-(z)}{\partial t} = -\Gamma_s P_- \left((\sigma_s^{abs} + \sigma_s^{em}) N_2 - \sigma_s^{abs} N_{tot} \right) - \Gamma_s N_2 \sigma_s^{em} \dfrac{2hc^2 \delta\lambda}{\lambda_s^3} \\ N_2 = \dfrac{\Gamma_p \sigma_p^{abs} P_p + \dfrac{\lambda_s}{\lambda_p} \Gamma_s \sigma_s^{abs} (P_s + P_+ + P_-)}{\Gamma_p (\sigma_p^{abs} + \sigma_p^{em}) P_p + \dfrac{\lambda_s}{\lambda_p} \Gamma_s (\sigma_s^{abs} + \sigma_s^{em}) (P_s + P_+ + P_-) + \dfrac{hc}{\lambda_p} \dfrac{A_{eff}}{\tau}} \end{cases} \tag{11}$$

This system is solved thanks to a classical Runge&Kutta Method with a shooting method to reach the counter-propagating ASE initial condition.

Such a technique leads to $\approx$ 10 mn only computation times to reach an accuracy better than 5% on the output pulse power compared to the effective output pulse power once the permanent regime is reached. This result was obtained for many amplifier configurations and input signals, using a Intel(R) Xeon(TM) CPU at 2.80 GHz without taking the advantage of any multiple-cores optimisation.

3.3 Simulation Results

Figure 3 and Figure 4 present the simulated propagation in the fibre (x-axis) versus the time (y-axis) for the excited state population and the pulsed signal, in the case of (fig. 3) a 10 ns-long pulse 77 ns-periodic signal, and (fig. 4) a 2 μs-long pulse 10 μs-periodic signal, both amplified thanks to a 40 cm-long fibre pumped with 2.5 W. The signal input peak power is 7 mW in both cases and its time shape is rectangular.

These simulations allow to observe the pulse width influence on the excited state population (fig. 3 and 4) and to predict the time shape of the amplified pulse (fig. 5) depending only on physical parameters.

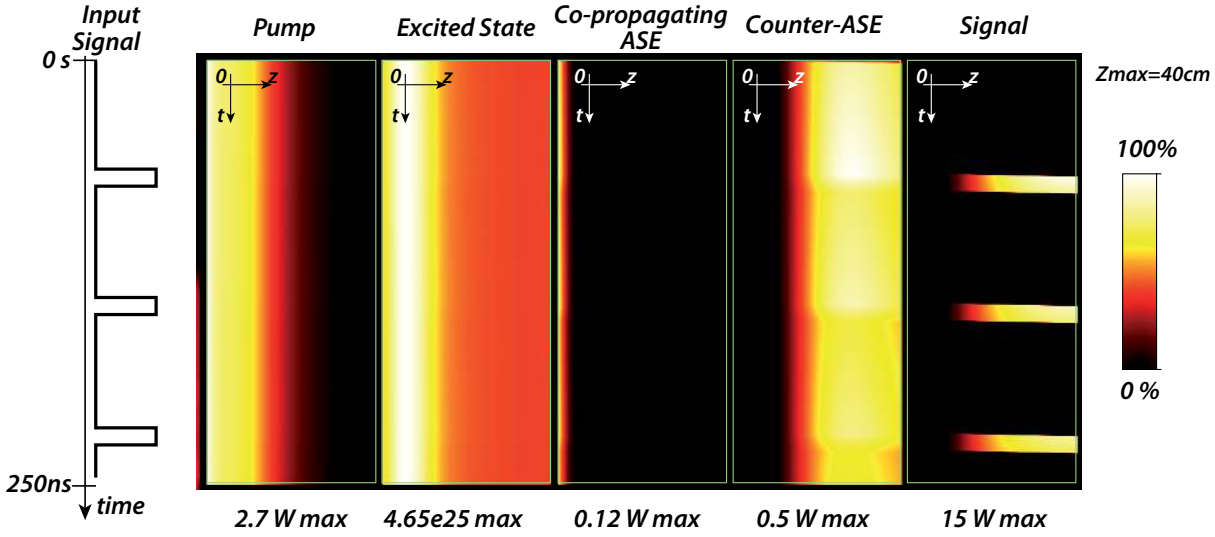

Figure 3. FDTD simulations of the optical amplifier with a short pulse at the input.

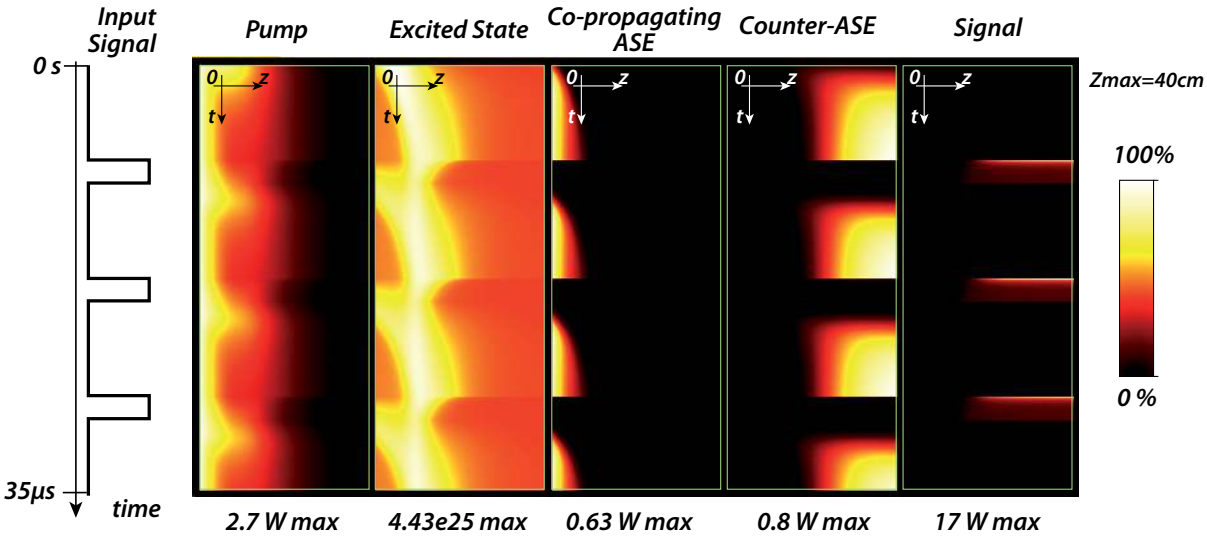

Figure 4. FDTD simulations of the optical amplifier with a long pulse at the input.

4. EXPERIMENTAL RESULTS COMPARED TO THEORY

4.1 Pulse shape and output power

For short enough pulses (shorter than about $\tau/1000$, where $\tau = 0.84\ ms$ is the excited state lifetime), we theoretically (fig. 3) and experimentally observe that the pulse does not decrease the population inversion and the pulse shape versus time is not modified. In this case, the peak power gain is close to a CW gain due to a CW input signal equal to the average value of signal in pulsed operation. With longer pulses, a gain decrease during the amplification can be observed (fig. 5), due to population inversion decrease (fig. 4).

In figure 6, the simulation is in good agreement with the experiment and describes correctly the amplification of pulses by the fibre.

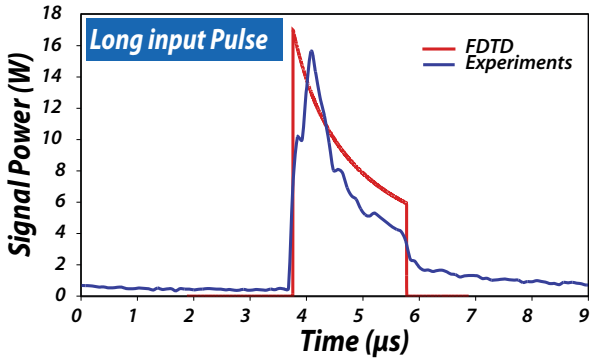

Figure 5. FDTD simulations vs experiments of the pulse dynamics : The 2 μs-long input pulse is amplified thanks to a 40cm-long fibre pumped with 2.5 W and average input signal power of 1.4 mW (7 mW peak).

4.2 Optical Gain compared to FDTD and CW model

For low average input signal powers, a parasitic laser oscillation due to residual reflections at the angle cleaved fibre ends appears and strongly decreases the gain applied to the pulsed input signal. Such a parasitic laser effect is also taken into account in the model.

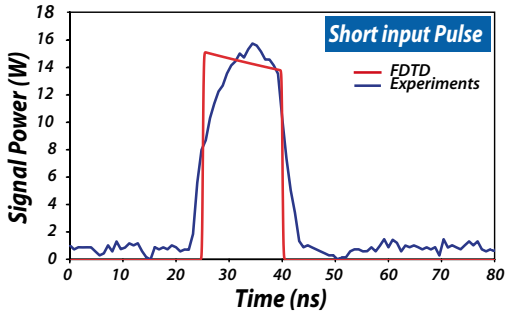

Figure 6. FDTD simulations vs experiments of the pulse dynamics : The 10 ns-long input pulse is amplified thanks to a 40cm-long fibre pumped with 2.5 W and average input signal power of 1.4 mW (7 mW peak).

We have experimentally measured the pulsed gain in a 40 cm-long fibre for a 2.5 W pump and many signal powers. To avoid pulse shape deformation during amplification, we used 10 ns pulses. We can see in fig. 7 the good agreement between the measured and simulated peak power gain.

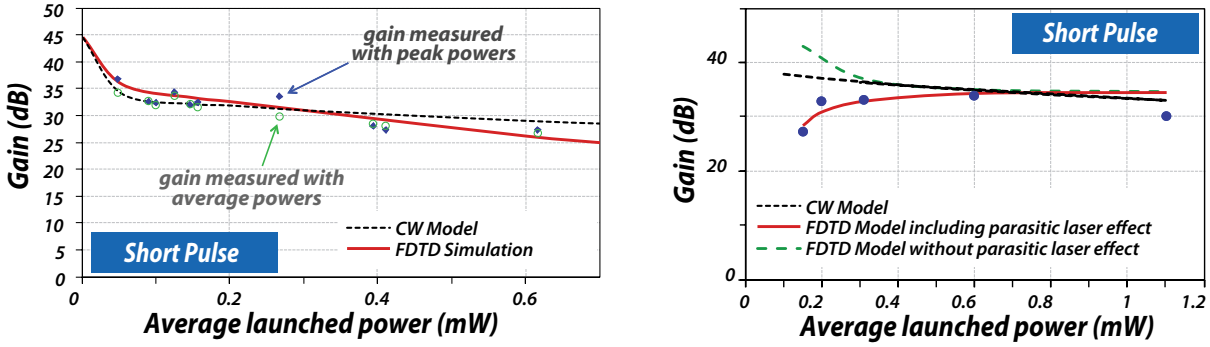

Figure 7. FDTD simulations vs experiments and steady-state model

Parasitic laser effects are limited for input average signal power higher than 0.3 mW. It appears with very low reflections such as the -60 dB reflection induced by a FC/APC connector. Without parasitic laser, gains higher than 30 dB can be obtained, and the temporal pulses shape and the signal spectrum are not modified. With an input average power of 1 mW, for a repetition rate of 13 MHz and pulses duration of 10 ns, the gain was 33 dB leading to an amplified average power of 2 W for a peak power of 14 W, which is in good agreement with the simulated peak power obtained in figure 3.

5. CONCLUSIONS

Pulsed signal amplification simulations taking into account both time and space evolutions and a parasitic laser effect describe correctly the experimental results. They show the evolution of the excited state population and can help to predict the amplifier performances in pulsed operation, and to choose the input pulses characteristics in terms of duration and repetition rates to optimize the peak power gain.

REFERENCES

[1] Birkin, D., Rafailov, E., Sokolovskii, G., Sibbett, W., Ross, G., Smith, P., and Hanna, D., "3.25 mw blue light by direct frequency-doubling of a 980-nm diode laser using an aperiodically-poled $LiNbO_3$ crystal," in [*Conference on Laser and Electro-Optics*], *OSA Technical Digest*, 425–426, Optical Society of America (2000).

[2] Raymond, T. D., Alford, W. J., Crawford, M. H., and Allerman, A. A., "Intracavity frequency doubling of a diode-pumped external-cavity surface-emitting semiconductor laser," *Optics Letters* **24**, 1127–1129 (1999).

[3] Bouchier, A., Lucas-Leclin, G., F.Balembois, and Georges, P., "Intense laser emission at 981 nm in an ytterbium-doped $KY(WO_4)_2$ crystal," in [*Advanced Solid State Photonics (20th Topical Meeting)*], TuB5, Optical Society of America (2005).

[4] Yiou, S., Balembois, F., Schaffers, K., and Georges, P., "Efficient laser operation of an Yb:S-FAP crystal at 985 nm," *Applied Optics* **42**, 4883–4886 (2003).

[5] Zou, S., Li, P., Wang, L., Chen, M., and Li, G., "980 nm Yb-doped single-mode fiber laser and its frequency-doubling with BIBO," *Applied Physics B* **95**, 685–690 (March 2009).

[6] Bouchier, A., Lucas-Leclin, G., Georges, P., and Maillard, J. M., "Frequency doubling of an efficient continuous wave single-mode Yb-doped fiber laser at 978 nm in a periodically-poled $MgO:LiNbO_3$ waveguide," *Optics Express* **13**, 6974 (August 2005).

[7] Selvas, R., Sahu, J. K., and Nilsson, J., "Q-switched 980 nm Yb-doped fiber laser," in [*Proceedings of CLEO*], 565 (2002).

[8] Okhotnikov, O. G., Gomes, L., Xiang, N., Jouhti, T., and Grudinin, A. B., "Mode-locked ytterbium fiber laser tunable in the 980-1070-nm spectral range," *Optics Letters* **29**, 1522 (September 2003).

[9] Hanna, D., Percival, R., Perry, I., Smart, R., Suni, P., and Tropper, A., "An ytterbium-doped monomode fibre laser: broadly tunable operation from 1.010 μm to 1.162 μm and three level operation at 974 nm," *Journal of Modern Optics* **37**, 517–525 (1990).

[10] Zenteno, L., Minelly, J., Dejneka, M., and Crigler, S., "0.65 W single-mode Yb-fiber laser at 980 nm pumped by 1.1W Nd:YAG," in [*Advanced Solid State Photonics*], Injeyan, H., Keller, U., and Marshall, C., eds., *OSA Trends in Optics and Photonics* **34**, 440–443, Optical Society of America (2000).

[11] Bouchier, A., Lucas-Leclin, G., and Georges, P., "Single-mode Yb-doped fiber laser at 980 nm for efficient frequency-doubling," *Advanced Solid-State Photonics* , 713 (2005).

[12] Boullet, J., Zaouter, Y., Desmarchelier, R., Cazaux, M., Salin, F., Saby, J., Bello-Doua, R., and Cormier, E., "High power ytterbium-doped rod-type three-level photonic crystal fiber laser," *Optics Express* **16**, 17891–17902 (September 2008).

[13] Röser, F., Jauregui, C., Limpert, J., and Tünnermann, A., "94 W and 980 nm high brightness Yb-doped fiber laser," *Optics Express* **16**, 17310 (October 2008).

[14] Soh, D., Codemard, C., Sahu, J. K., Nilsson, J., Philippov, V., Alegria, C., and Jeong, Y., "A 4.3W ytterbium-doped jacketed air-clad-fiber amplifier," in [*Advanced Solid State Photonics (19th Topical Meeting)*], MA3, Optical Society of America (2004).

[15] Digonnet, J. F., [*Rare-Earth-Doped Fiber Lasers and Amplifiers*], Marcel Dekker (2001).

[16] Marcuse, D., "Pulsing behavior of a three-level laser with saturable absorber," *IEEE Journal of Quantum Electronics* **29**, 2390 (August 1993).

[17] Press, W. H., Teukolsky, S. A., Vetterling, W. T., and Flannery, B. P., [*Numerical Recipes in C - The Art of Scientific Computing - Second Edition*], Academic Press (1980).

[18] Courant, R., Friedrichs, K., and Lewy, H., "On the partial difference equations of mathematical physics," *IBM Journal* (March 1967).